NeuroImage 300 (2024) 120789

Contents lists available at ScienceDirect

NeuroImage

journal homepage: www.elsevier.com/locate/ynimg

The critical mediating roles of the middle temporal gyrus and ventrolateral prefrontal cortex in the dynamic processing of interpersonal emotion regulation

Jiazheng Wang [a], Zhenzhen Yang [a], Benjamin Klugah-Brown [a], Tao Zhang [d], Jiemin Yang [b], JiaJin Yuan [b,**], Bharat B Biswal [a,c,*]

[a] The Clinical Hospital of Chengdu Brain Science Institute, MOE Key Laboratory for Neuroinformation, Center for Information in Medicine, School of Life Science and Technology, University of Electronic Science and Technology of China, Chengdu, China
[b] Sichuan Key Laboratory of Psychology and Behavior of Discipline Inspection and Supervision, Institute of Brain and Psychological Science, Sichuan Normal University, Chengdu, Sichuan 610041, China
[c] Department of Biomedical Engineering, New Jersey Institute of Technology, Newark, NJ 07102, United States
[d] Mental Health Education Center, Xihua University, Chengdu, China, 610039

ARTICLE INFO

Key words:
Interpersonal emotion regulation (IER)
Dynamic functional connectivity (DFC)
Middle temporal gyrus (MTG)
Ventrolateral prefrontal cortex (VLPFC)

ABSTRACT

Interpersonal emotion regulation (IER) is a crucial ability for effectively recovering from negative emotions through social interaction. It has been emphasized that the empathy network, cognitive control network, and affective generation network sustain the deployment of IER. However, the temporal dynamics of functional connectivity among these networks of IER remains unclear. This study utilized IER task-fMRI and sliding window approach to examine both the stationary and dynamic functional connectivity (dFC) of IER. Fifty-five healthy participants were recruited for the present study. Through clustering analysis, four distinct brain states were identified in dFC. State 1 demonstrated situation modification stage of IER, with strong connectivity between affective generation and visual networks. State 2 exhibited pronounced connectivity between empathy network and both cognitive control and affective generation networks, reflecting the empathy stage of IER. Next, a 'top-down' pattern is observed between the connectivity of cognitive control and affective generation networks during the cognitive control stage of state 3. The affective response modulation stage of state 4 mainly involved connections between empathy and affective generation networks. Specifically, the degree centrality of the left middle temporal gyrus (MTG) mediated the association between one's IER tendency and the regulatory effects in state 2. The betweenness centrality of the left ventrolateral prefrontal cortex (VLPFC) mediated the association between one's IER efficiency and the regulatory effects in state 3. Altogether, these findings revealed that dynamic connectivity transitions among empathy, cognitive control, and affective generation networks, with the left VLPFC and MTG playing dominant roles, evident across the IER processing.

1. Introduction

In daily life, receiving comfort and social support from friends, family members, or even strangers can facilitate emotional release, especially when we are experiencing negative emotions. This process of altering emotional states in social interaction is referred to as interpersonal emotion regulation (IER; Butler, 2011; Hofmann, 2014; Zaki, 2020). Zaki and Williams propose a framework for IER that features a "regulator" who supports a "target" in their endeavor to down-regulate negative emotions (Zaki & Williams, 2013). The key distinction of Interpersonal Emotion Regulation (IER) lies in its emphasis on the intentional efforts made by the regulator to modify the emotional experience of the target in the social interaction context, as opposed to self-emotion regulation. For instance, during childhood, our negative emotions (as the target) are often influenced by our parents (as the regulators; Butler, 2011; Xie et al., 2016; Zaki, 2020). It has long been emphasized that IER forms the foundation for individuals to manage their emotions by themselves (Xie et al., 2016; Zaki, 2020). Indeed, IER

* Corresponding author at: No. 2006 Xiyuan Street, Chengdu 610041, China.
** Corresponding author at: No. 5 Jingan Street, Chengdu 610041, China.
E-mail addresses: yuanjiajin168@126.com (J. Yuan), bbiswal@gmail.com (B.B. Biswal).

https://doi.org/10.1016/j.neuroimage.2024.120789
Received 21 April 2024; Received in revised form 30 July 2024; Accepted 12 August 2024
Available online 17 August 2024

is beneficial for individuals in establishing well-conditioned social relationships and prosocial behaviors. Crucially, disturbance in IER is vital hallmark of various affective disorders, such as depression and borderline personality (Dixon-Gordon et al., 2015; Zaki, 2020). Therefore, understanding the cognitive and neural substrates of IER can provide valuable insights into potential biomarkers and treatments for affective disorders.

Functional neuroimaging and computational neural models implicate multiple brain regions and networks in IER (Coan et al., 2006; Morawetz et al., 2021; Reeck et al., 2016; Zhang et al., 2023). The most comprehensive meta-analysis on neural investigations of IER reveals distinct brain networks associated with this cognitive processing, including the empathy network, the cognitive control network, and the affective generation network (Reeck et al., 2016). For the target, the empathy network activates to perceive affective states and comprehend the regulatory information provided by the regulator, involving areas such as the temporal parietal junction (TPJ), dorsal medial prefrontal cortex (DMPFC), and middle temporal gyrus (MTG; Jauniaux et al., 2019). Meanwhile, the cognitive control network largely overlaps with the frontal-parietal network, including regions like the dorsolateral prefrontal cortex (DLPFC), ventrolateral prefrontal cortex (VLPFC), and the inferior parietal gyrus (IPG). These areas are responsible for directing attention to goal-oriented features and maintaining regulatory goals (Ochsner et al., 2012). The affective generation network primarily encompasses the limbic network, which mainly includes the insula and amygdala, regions believed to process affective experiences (, Gao et al., 2021).

To date, numerous investigations on emotion regulation have focused on various aspects of functional connectivity to elucidate the neural mechanisms underlying the regulation processing (Fang et al., 2020; Morawetz et al., 2020). For instance, the activity of the cognitive control network exerts a modulatory effect on the affective generation network, resulting in the down-regulation of negative emotions (Fang et al., 2020; Zhao et al., 2020). Furthermore, studies on patients with major depression disorder and borderline personality disorder have shown disrupted activation in the frontal cortex during emotion regulation processing, which subsequently affects functional connectivity with the affective generation regions (Johnstone et al., 2007; Koenigsberg et al., 2009). However, the connectivity associations between these brain networks during the IER processing remain unclear. This study utilized IER task-based functional magnetic resonance imaging (fMRI) and functional connectivity analyses to describe the neural substrates of the IER processing.

Functional connectivity (FC) evaluates the temporal coupling among different brain regions (Gao et al., 2021). It describes brain regions associations for both stationary and dynamic temporal levels. For the stationary functional connectivity (sFC), a common practice is to compute the Pearson's correlation coefficient between signals from two brain regions, resulting in a single correlation value per pair of regions that remains constant over time (Liang et al., 2021). Conceptually, the sFC represents the total correlation between two regions, while dynamic FC (dFC) assesses the variability of information transfer (Schoonheim et al., 2021). The dFC reveals intermittent and variations in connectivity over time that might be obscured by sFC (Douw et al., 2020). Together, these measures offer unique insights into brain regions functioning essential for the cognitive processing (Bertolero & Bassett, 2020; Schoonheim et al., 2021). Both sFC and dFC analyses provide complementary information when examining brain functional connectivity. Therefore, profiling both types of connectivity in the IER processing could be beneficial for enhancing social functions and aiding recovery from emotion regulation deficiency disorders.

With the advancement of dynamic functional connectivity, there's growing interest in investigating the temporal characteristics of brain activity (Liang et al., 2021). This dynamic approach employs a sliding window, allowing for the identification of multiple discrete connectivity states, characterizing these connectivity states. For example, Feng and colleagues have identified four distinct brain states and revealed that the cortical mechanism underlying cognitive reappraisal follows a 'top--down' pattern during the processing of emotion regulation (Fang et al., 2020). Meanwhile, the graphic theoretical measures can extract key hubs from complex connections including betweenness centrality, degree centrality and node efficiency. Betweenness centrality quantifies the number of shortest paths through which a given brain region serves as a crucial hub for connecting different networks. It is commonly used in fMRI network analysis to determine the significance of a brain region based on its role as a central "connector" between other regions (Raghavan Unnithan et al., 2014). The identification of the specific DLPFC region plays a pivotal role in facilitating the connectivity structures underlying various affective states and subsequent regulatory efforts, as indicated by its high betweenness centrality (Fang et al., 2020). Degree centrality indicates the number of functional connections a brain region has, regions with high degree centrality are considered vital for information transmission within the network because they have more direct connections to other regions, facilitating efficient information flow across the network (Zhang et al., 2016). Node efficiency measures the degree to which nodes in a network form tightly interconnected clusters or modules, reflecting the level of interconnectivity between a node's neighbors. Brain regions with high node efficiency are deemed essential for specialized processing within localized functional networks (Wang et al., 2017). However, our understanding is limited regarding the diversity of brain networks and the characteristics of connectivity states throughout the IER processing. This study was motivated by this gap in literature.

The present study employed an IER task functional MRI (fMRI) experiment (Wang et al., 2023; Xie et al., 2016). This experimental paradigm employed visual stimuli, emotional images designed to evoke aversive emotions, with the aim of eliciting robust and reliable neural activation patterns in a cohort of healthy individuals. Following the induction of negative emotions, the experimenter acted as the regulator either regulated the participants' emotions (the target) by implementing the reappraisal strategy, or instructed them to simply observe the negative emotional pictures without altering their emotional state. To mimicry a daily social setting, all the emotional regulation instructions were delivered via short video clips featuring the regulator. Contrasting the whole stage allowed us to identify the functional network connectivity of the dynamic processing of IER. The aims of this study are three-fold. First, we aim to dissect the specific functional connectivity during the IER processing. To accomplish this goal, we employed both sFC and dFC approaches as robust methodologies for integrating the stationary and time-varying neural substrates of the IER. Second, we intend to use the betweenness centrality, degree centrality and node efficiency as metrics for characterizing the distinctive features of each brain state in terms of sFC and dFC. Lastly, our focus lies in the integration of behavioral performance and functional connectivity, with the aim of identifying key regions that facilitate connectivity in IER and elucidating the cognitive-neural substrates underlying the IER processing.

2. Methods

2.1. Participants

The present study included fifty-five healthy adult participants (26 females and 29 males) between 18-22 years of age (mean age = 20.5, standard deviation = ± 1.96). The participants were right-handed, had normal or corrected visual acuity, and reported no familial history of psychiatric, neurological, or affective disorders. The study was approved by the local ethics committee of the University of Electronic and Scientific Technology of China, and informed consent was obtained from all participants who also received financial compensation.

2.2. Questionnaire

We obtained interpersonal regulation questionnaire (IRQ) to assess the regular usage of IER to comprehensive the IER investigation. The IRQ contains two subscales of IRQ tendency and IRQ efficiency to detect one's tendency to use IER as well as the efficiency of IER effect (Williams et al., 2018).

2.3. Data acquisition

The task-fMRI image was acquired using an 8-channel phased-array head coil on a 3.0-T GE Discovery MR750 system (General Electric Medical System, Milwaukee, WI, USA). All images were obtained using a single-shot simultaneous multi-slice (SMS) or multiband (MB) gradient-echo EPI sequence with the following parameters: echo time (TE) = 30 ms, repetition time (TR) = 2000 ms, flip angle = 90°, spacing between slices = 3 mm, field of view (FOV) = 240 mm × 240 mm, acquisition matrix = 64 × 64, slice thickness = 3 mm, slice number = 42.

2.4. Interpersonal emotion regulation task

To create a social context, the present study instructed the experimenter to act as the regulator guiding the participants (the targets) to decrease their negative emotions in reappraisal strategy. Inspired previous studies, we applied a reappraisal-IER task to assessed the individual's IER (Ochsner et al., 2004; Xie et al., 2016).

This study used a within-subjects design, consisting of two conditions: IER condition and watch condition. The two conditions were in different runs, with each run consisting of 20 trials. The timeframe of each trial included 6 steps: (1) a fixation presented for 1 second (s); (2) a 4 s preparation phase; (3) the participants watched a 7 s video clip, in which participants were guided on how to use the reappraisal strategy to down-regulate their negative emotions (IER condition) or experiencing the following negative emotional pictures (Watch condition); (4) a jitter randomized from 1 s - 3 s; (5) a negative emotional picture displayed for 7 s. For this phase, participants needed to memorize the reappraisal strategy (mentioned in former video clip) to reduce their negative emotions (IER condition) or by simply experiencing their emotions (Watch condition); (6) the participants rated their negative emotional ratings on a 5-point scale ranging from 0 (not at all negative) to 4 (very negative) in 3 s. More details see Fig. 1. The negative emotional rating serves as a behavioral indicator of emotional regulatory performance, with the watch condition serving as the baseline for emotional regulation. Therefore, the difference in emotional ratings between the IER condition and watch condition represents the IER effects.

The task was block design, consisting of two runs, each comprising 20 trials, with a duration of 440 s for each run. The 40 pictures in the 40 trials were picked from the international affective picture system (IAPS) and open affective standardized image set (OASIS, Benedek, 2017; with the picture numbers shown in supplementary materials). To ensure comparable emotional arousal and valence across the two conditions, we employed the standardized ratings of each emotional picture from IAPS and OASIS to assess the 40 pictures in both conditions. There was no significant difference in arousal [t (1, 38) =.162, p = .872] and valence [t (1, 38) = -1.105, p = .276] in the two conditions.

2.5. Preprocessing

The fMRI data was preprocessed using the DPABI (V3.1) toolbox (http://www.rfmri.org/dpabi) in the Matrix Laboratory software (MATLAB 2018a, https://ww2.mathworks.cn/en/products/matlab). The following steps outline the procedures: 1) the first five volumes have been removed; 2) sliced timing correction; 3) realignment; 4) spatial normalization by EPI template; 5) smoothed with a Gaussian kernel (FWHM = 8 mm). Two participants were excluded from data analysis due to head motion exceeding 2 mm or 2° during the IER condition.

2.6. Group Independent component analysis (gICA)

The preprocessed fMRI data from both IER and watch conditions underwent high-model order group independent component analysis (gICA) with the GIFT toolbox (http://mialab.mrn.org/software/gift/). Independent components (ICs) are estimated from the fMRI data using the minimum description length criteria. The Infomax algorithm repeated 20 times in ICASSO in other to identify stable and consistent components. Finally, 30 ICs were generated under the automated anatomical labeling atlas (AAL). The 30 peak coordinates for all the ICs was utilized as gICA spatial map for further analysis (Klugah-Brown et al., 2019; Zhang et al., 2016).

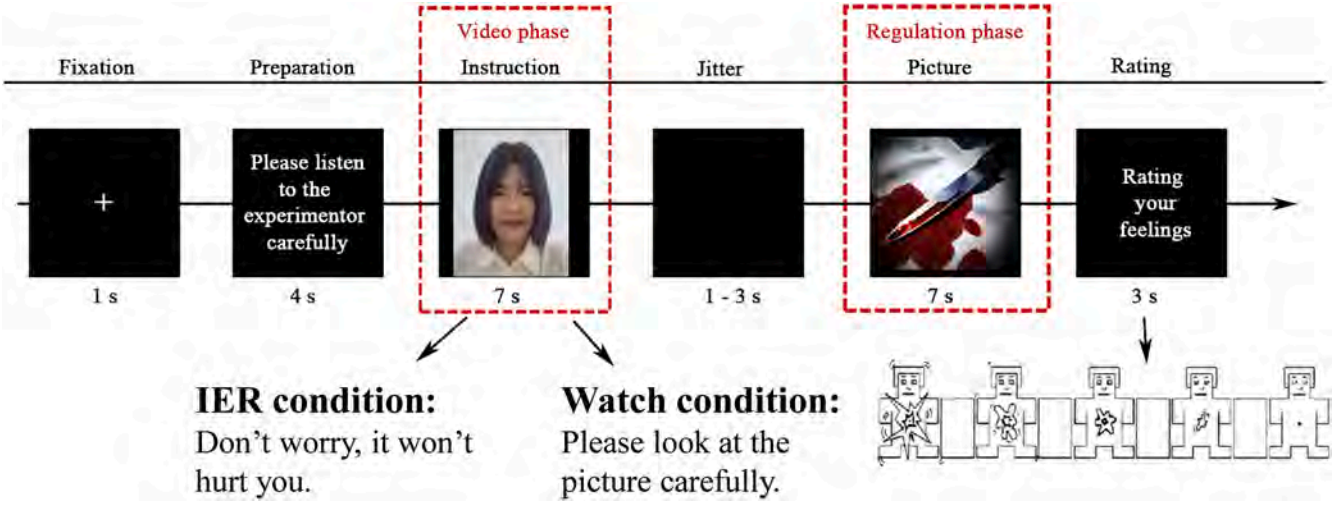

Fig. 1. The timeframe of the IER task, the task contains 2 conditions: IER condition and Watch condition. The IER condition instructed subjects to down-regulate their negative feelings in reappraisal strategy. The Watch condition required subjects to look at the negative pictures and experience their feelings. The trials involved the presentation of a fixation cross, a preparation and instruction phases, a jitter with varying inter-trial intervals (1 - 3 s), a negative picture, and a rating scale. The instruction was a 7 s video clip, in which the regulator (the experimenter) who regulated participants' emotions by using reappraisal strategy, or told participants to look at and respond naturally to the pictures, depending on the condition.

2.7. Functional Connectivity

2.7.1. Stationary functional connectivity (sFC)

To quantify IER processing, the preprocessed data underwent a first-level analysis for each participant under different conditions. This analysis used a General Linear Model based on blood oxygen level dependent (BOLD) signals. Six head motion parameters, all stimuli (e.g., fixation) for each condition were convolved with the hemo-dynamic response function, and high-pass filter was 128 s in Statistical Parametric Mapping 12 (SPM 12) (https://www.fil.ion.ucl.ac.uk/spm/software/spm12/).

The peak coordinates of ICs in the GICA spatial map were utilized as regions of interest (ROIs) to perform Pearson correlation on a ROI-wise by averaging over the entire time series in both IER condition and Watch condition, resulting in two ICs × ICs × participants matrices. As the watch condition was the baseline of the emotion regulation processing, the present study utilized IER correlation matrix minus watch correlation matrix (IER-Watch) to obtain the specific IER processing. The functional connectivity of each IC utilized Pearson correlation coefficient (r value). These r values were then transformed into normalized Z-scores. Therefore, The ICs × ICs × participant matrix of IER-watch matrix profiled the sFC of the IER processing.

2.7.2. Dynamic functional connectivity (dFC) and network properties

Sliding window was performed to measure the dFC using the GIFT toolbox (http://mialab.mrn.org/software/gift/), based on the gICA spatial map. It has been emphasized that the sliding window length range from 30 s to 60 s is feasible for assessing cognitive state in resting data (Allen et al., 2014; Hutchison et al., 2013; Nomi et al., 2016). Also, the sliding window correlation analysis ensures a window range 30 s to 240 s could be used in multiple task fMRI data (Bassett et al., 2011; Hutchison et al., 2013). The present study utilized several window length (15TR, 20 TR, 25 TR, 30 TR, 35TR, 40 TR, 45 TR, respectively), and step size of 1TR to estimate a stabilized window length. Next, these group-level matrix of windows × ICs × ICs were input into the k-means clustering algorithm, separately. The goal was to decompose and profile the character of the FC of the IER processing. The k-means algorithm generated a discrete set of cluster. The optimal number of clusters (k) was determined using the elbow criterion (Zhang et al., 2016). To minimize the risk of converging to local minima, the clustering algorithm ran 2000 iterations with randomly initialized centroid positions. Centroids from the group-level clusters initialized the clustering of each participant's window matrix. All the windows length (15TR, 20 TR, 30 TR, 35TR, 40 TR, 45 TR) generated 4 clusters, except for 25TR (which generated 5 clusters, Fig. 3). It implied that there were 4 stationary brain states in the IER processing. Therefore, we chose the averaged window length of 30TR and 1TR step, which generated 195 windows to detail the dFC of the IER processing. This resulted in definitive cluster centroids and brain state for the IER processing (Allen et al., 2014). After that, we employed betweenness centrality, degree centrality, and node efficiency to profile the property of the positive and negative connections in sFC and dFC.

Furthermore, the transition state vectors were obtained through the calculated membership assignments for all windows. Then, we utilized the transition state vectors derived from the dynamic FNC matrices of the windows of the IC time courses to calculate the dwell time in each state, which refers to the number of successive windows spent in the same state.

2.8. Associations between graphic theoretical properties of sFC/dFC and behaviors

After characterizing each brain state, we employed Pearson correlation and mediation analysis to examine the association between neural properties and behavioral performance of the IER processing. Mediation analysis was conducted using the standard 3-variable path model and assessed through a bootstrap test to examine the relationships among three variables (Menatti et al., 2015; Wager et al., 2008; Wang et al., 2023). The models were assessed using the SPSS macro PROCESS, which employs bootstrap estimation to calculate the indirect effect between the independent and dependent variables, along with an estimated standard error and 95 % confidence intervals (CI) for the population value of this indirect effect. The indirect effects were estimated through bootstrap resampling with 5000 iterations. Before performing the analyses, all variables were standardized by z-scoring in order to derive standardized β weights.

3. Results

3.1. Manipulation check

The post-experimental interview confirmed that all participants held the belief the regulator was physically present in an adjacent observation room throughout the scanning process. They actively engaged in the task by following the guidance provided by the regulator.

3.2. Emotional responding

We employed paired sample *t*-test with conditions type (IER and watch) as a within-participants factor to test whether the task elicited IER successfully. The participants reported significantly experiencing fewer negative affect for IER condition ($M = 2.12$, $SD = 0.78$, $t\ (54) = 4.498$, $p < 0.0001$, 95 % CI [.1977, .5156], Cohen's d = 0.61) compared to watch condition ($M = 2.47$, $SD = 0.67$) (Fig. 4a). The emotional rating by the participants was the emotional response of the IER and watch condition as behavioral data of IER, and thus, the emotional response variations between IER and watch conditions was the behavioral indictors of IER effect.

3.3. gICA and sFC

The gICA results produced 30 distinct ICs, they were selected based on peak activation clusters in the grey matter with little or no overlap within the white matter and other areas, such as the edges of the brain and ventricles; this was done through the inspection of spatial maps (Kuang et al., 2024). These ICs were then mapped into the next functional connectivity analysis based on their peak coordinates, as detailed in Table 1. The sFC is demonstrated in Fig. 4b. Notably, these results revealed strong positive correlations within the frontal-parietal lobe, temporal lobe and central cortex (More connectivity details see Table 1 and Fig. 2c).

3.4. Clustering results

In our study, the range of variation of k set in elbow method is 2-10 to optimally capture dynamic states. For the optimal k value of k-means algorithm, there are some methods to be selected, such as elbow, silhouette, gap statistic method. In particular, previous studies have shown that the elbow method is a very stable state selection method and has been widely used in FNC research (Fang et al., 2020; Klugah-Brown et al., 2019; Nomi et al., 2016). For better comparison, we also assessed the state selection using the silhouette and gap statistic methods and the results showed that the number of states is less than 3 (k = 2 in silhouette method, k=1 in gap statistic method; Fig. s1 in supplementary materials). Such a small number of states may ignore some important information and make it difficult to satisfy the subsequent results. Whiles, more clusters will give more interacting FC among states and can be used to find abnormal functions during processing of interpersonal emotion regulation. Inspired by previous studies (Fang et al., 2020; Klugah-Brown et al., 2019; Nomi et al., 2016), we chose the elbow results to determine the optimal number of states in our study.

Table 1
The independent components (ICs) of group independent components analysis (GICA) in interpersonal emotion regulation condition (IER) and Watch condition.

ICs	Abbreviations	MNI			Brain regions
		x	*y*	*z*	
01	DLPFC_L	*-51*	*20*	*2*	Inferior frontal cortex, triangular part
02	DLPFC_R1	*51*	*20*	*26*	Inferior frontal cortex, triangular part
03	DLPFC_R2	*30*	*53*	*23*	Middle frontal cortex
04	VLPFC_L	*-33*	*56*	*-4*	Superior frontal cortex, medial orbital part
05	DMPFC_L1	*0*	*26*	*38*	Superior Medial frontal cortex
06	DMPFC_L2	*0*	*59*	*17*	Superior Medial frontal cortex
07	VMPFC_L	*0*	*41*	*-16*	Gyrus rectus
08	CUN_L	*0*	*-82*	*17*	Cuneus
09	CUN_R	*3*	*-82*	*35*	Cuneus
10	CAL_L	*0*	*-88*	*-7*	Calcarine
11	SOG_R	*12*	*-97*	*20*	Superior Occipital gyrus
12	MOG_L	*-39*	*-82*	*32*	Middle Occipital gyrus
13	IOG_L	*-27*	*-97*	*-10*	Inferior Occipital gyrus
14	STG_L	*-60*	*5*	*-4*	Superior Temporal gyrus
15	STG_R	*57*	*-22*	*14*	Superior Temporal gyrus
16	MTG_L	*-57*	*-19*	*2*	Middle Temporal gyrus
17	MTG_R	*60*	*-49*	*5*	Middle Temporal gyrus
18	ITG_R	*51*	*-70*	*-4*	Inferior Temporal gyrus
19	SPTG_L	*-42*	*2*	*-16*	Superior Pole Temporal gyrus
20	MPTG_L	*-36*	*8*	*-31*	Middle Pole Temporal gurus
21	FEF_R	*42*	*-22*	*65*	Frontal eye fields
22	PTCG_L1	*-42*	*-40*	*62*	Postcentral gyrus
23	PTCG_L2	*-57*	*-10*	*23*	Postcentral gyrus
24	PACG_R	*6*	*-37*	*77*	Paracentral gyrus
25	SMA_L	*0*	*20*	*50*	Supplementary Motor Area
26	SPG_R	*27*	*-76*	*50*	Superior Parietal gyrus
27	IPG_L	*-57*	*-34*	*44*	Inferior Parietal gyrus
28	TPJ_L	*-39*	*-73*	*44*	Temporal Parietal junction
29	TPJ_R	*48*	*-64*	*41*	Temporal parietal junction
30	INS_R	*42*	*8*	*-4*	Insular

Note: DLPFC (dorsolateral prefrontal cortex); VLPFC (ventrolateral prefrontal cortex); VMPFC (ventromedial prefrontal cortex); DMPFC (dorsomedial prefrontal cortex); L (left); R (right); ICs (independent components).

3.5. dFC and network properties of each states

The clustering and dFC results revealed four distinct brain states in the IER processing. To obtain the representative network for each state, we extracted its centroid point. Then, for each of the four centroid points, we referenced the number of the time window back to every participant to pinpoint significant connectivity through one simple t-test with FDR ($p < 0.01$). The group-specific representations of the four brain states are depicted in Fig. 2e. State 1 mainly showed negative connectivity of the bilateral occipital lobe with the left MTG and the left TPJ. The positive connectivity were found between the right insula (INS) and the right cuneus (CUN)/ the left middle occipital gyrus (MOG); the left dorsolateral prefrontal cortex (DLPFC) and the left MTG. The occipital lobe served as the central region, with a particular emphasis on the right CUN exhibiting a high degree of centrality and node efficiency, the left calcarine demonstrated elevated betweenness centrality in positive connections. While the bilateral MTG showed high betweenness centrality, degree centrality and node efficiency in negative connections of this brain state. The State 2 exhibited high centrality within the temporal lobe, central and parietal lobe. It primarily revealed negative connectivity between the bilateral middle temporal gyrus (MTG) and the bilateral temporal parietal junction (TPJ), alongside positive connectivity between left MTG and the left superior parietal gyrus (SPG). The left MTG exhibited a high betweenness centrality in positive connections, while as the right MTG showed high degree centrality and node efficiency in negative connections of this state.

The State 3 displayed dominant negative connectivity between the left ventrolateral prefrontal cortex (VLPFC) and the left ventromedial prefrontal cortex (VMPFC), along with positive connectivity between the bilateral superior temporal gyrus (STG) and the left DLPFC/ VMPFC; as well as the positive connections within the right frontal eye fields (FEF) and the left VMPFC/ the right DLPFC. Additionally, the frontal cortex exhibited prominent central hubs, particularly the left VLPFC, which demonstrated high degree centrality in negative connections of this state. State 4 predominantly exhibited positive connectivity between the bilateral TPJ and the right DLPFC/ the left SPG. Additionally, the bilateral TPJ demonstrated negative connectivity with bilateral MTG/ the left STG, as well as negative connectivity between the right INS and the right inferior temporal gyrus (ITG). Furthermore, the right MTG exhibited high betweenness centrality in negative connections of the State 4. More connectivity details see Table 2, Figs. 2e and 5.

The states in the present study showed continuously distribute (Fig. 7), and these states contain 32, 30, 61, 72 windows, respectively. Thus, these functional connectivity states could be viewed as effective. Dwell time (number of successive windows in the same state) and states transition number (number of transition for dynamic brain states) showed in Fig. 7.

3.6.1. Pearson correlation analysis

In negative connections of sFC, the betweenness centrality of the left DMPFC showed a positive correlation with IRQ_T ($r = 0.37$, $p = 0.0079$). In positive connections of sFC, the betweenness centrality of left VMPFC ($r = -0.36$, $p = 0.0103$) and degree centrality of left DMPFC ($r = -0.34$, $p = 0.0149$) had negative correlation with emotional rating of watch condition – IER condition; the node efficiency of the left TPJ showed positive correlation with emotional rating ($r = 0.35$, $p = 0.0282$), see Fig. 4d.

For the negative connections of dFC, the degree centrality of the left MTG in state 2 showed negative correlation with IRQ_T ($r = -0.27$, $p = 0.0443$), and positive correlation with emotional rating ($r = 0.34$, $p = 0.0168$). The betweenness centrality of the right TPJ showed negative correlation with emotional rating ($r = -0.37$, $p = 0.0074$), see Fig. 6. For the positive connections of dFC in state 2, the node efficiency of the left MTG had negative correlation with emotional rating ($r = -0.34$, $p = 0.0151$), and the node efficiency of the right FEF had positive correlation with emotional rating ($r = 0.37$, $p = 0.0077$). In state 3, the node efficiency of the left MTG showed positive correlation with IRQ ($r = 0.38$, $p = 0.0043$). Meanwhile, the betweenness centrality of the left VLPFC showed positive correlation with emotional rating ($r = 0.30$, $p = 0.0401$) and IRQ_E ($r = 0.36$, $p = 0.0071$) as shown in Fig. 6.

3.6.2. Mediation analysis

The mediation analysis showed the degree centrality of the left MTG in state 2 mediated the correlation between emotional rating and IRQ_T (indirect path a = -0.2723; indirect path b = 0.2623, total relationship c = 0.1667, direct path c' = 0.2381; 95 % bootstrap confidence interval (CI) = [0.0078, 0.1859]; effect size = 42.83 % (Fig. 8). The degree centrality of the left VLPFC in state 3 mediated the correlation between emotional rating and IRQ_E (indirect path a = 0.4178; indirect path b = 0.5040, total relationship c = 0.0105, direct path c' = -0.2001; 95 % bootstrap confidence interval (CI) = [0.0769, 0.4512]; effect size = 20.06 % (Fig. 8). Zero does not appear in the CI, which demonstrated a significant mediation effect for the mediating factor.

4. Discussion

In the present study, combining the behavioral performance and brain connectivity revealed the dynamic cognitive-neural substrate of the IER processing. The negative emotional rating in the IER condition was significantly lower compared to that in the watch condition, indicating successful induction of IER in this study. Furthermore, both sFC and dFNC analyses were utilized to assess the IER-related networks transition, emphasizing its temporal properties across different brain states. The sFC revealed strong connectivity from the empathy network to both the cognitive control network and the affective generation

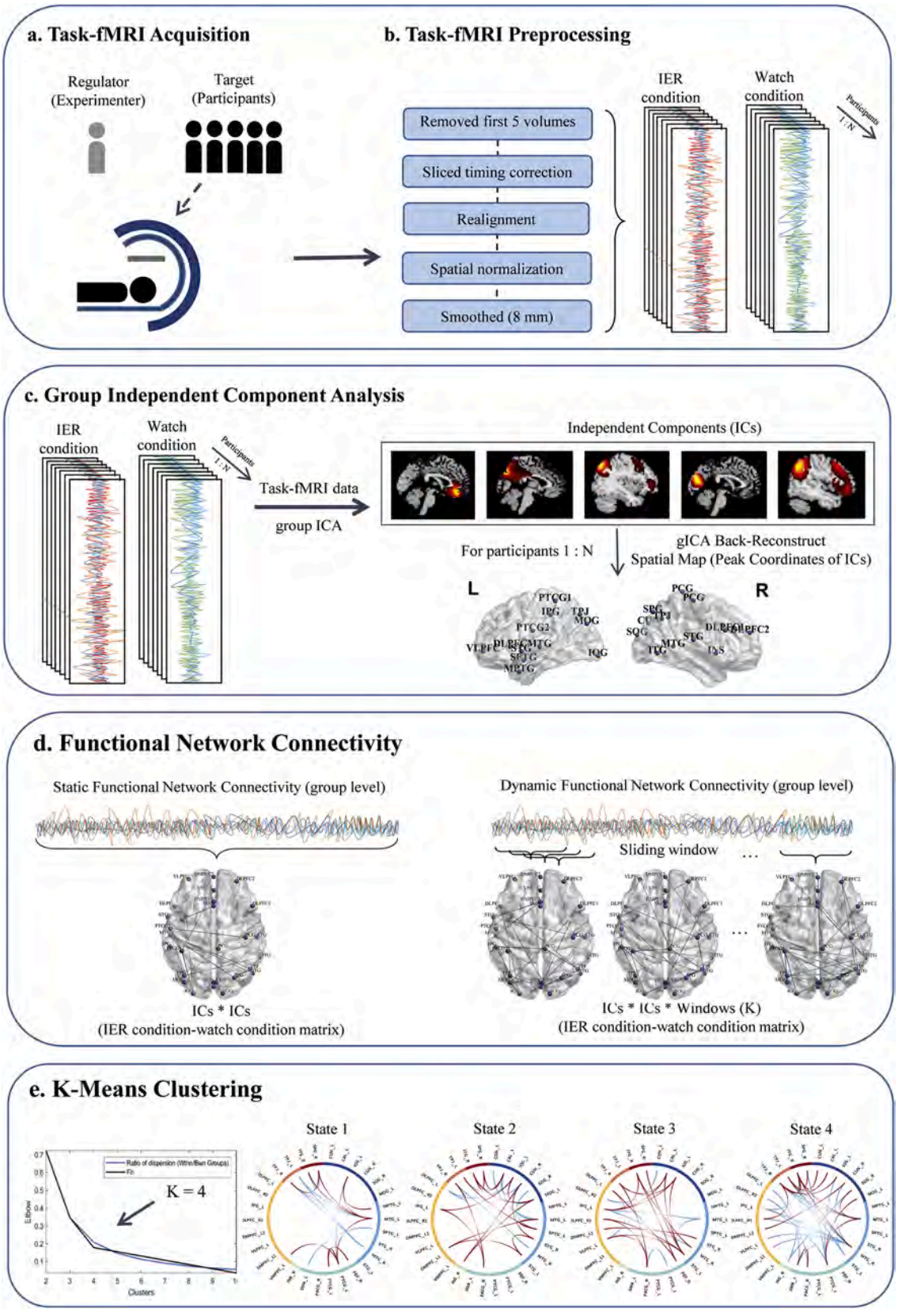

(caption on next page)

Fig. 2. The pipeline of the entire work. a: fMRI data Acquisition, the participant in the present study was the target, who was guided by the regulator (the experimenter) to decrease their negative emotions. After the participant understood the task, they would be conducted the formal task in scanner to record their neural activity during IER task. b: fMRI data Preprocessing, The IER condition and watch condition data were preprocessed in DPABI toolbox. c: Group Independent Component Analysis, the method decomposed the functional parcellation of the brain resulting into several independent components (ICs) in gift toolbox. After the ICs generated, the peak coordinates of the ICs would be collected into the gICA spatial map for following analysis. d: Functional Network Connectivity, the IER condition and watch condition were calculated by Parson correlation under the gICA spatial map, separately, and got two ICs * ICs * participants matrices. Then, we used IER correlation matrix minus watch condition (baseline) for next sFC and dFC analysis. The dynamic analysis utilized Gauss-sliding windows (15TR, 20TR, 25TR, 30TR, 35TR, 40TR, 45TR) in 1TR steps to acquire 195 correlation matrices in group level, generating ICs × ICs × windows matrices. e: K-means clustering, The K-means clustering would show the classified states of those matrices, and the elbow criterion generated stable clusters with K = 4. The four circle Fig.s showed significant dFC of the IER processing (FDR, $p<0.01$).

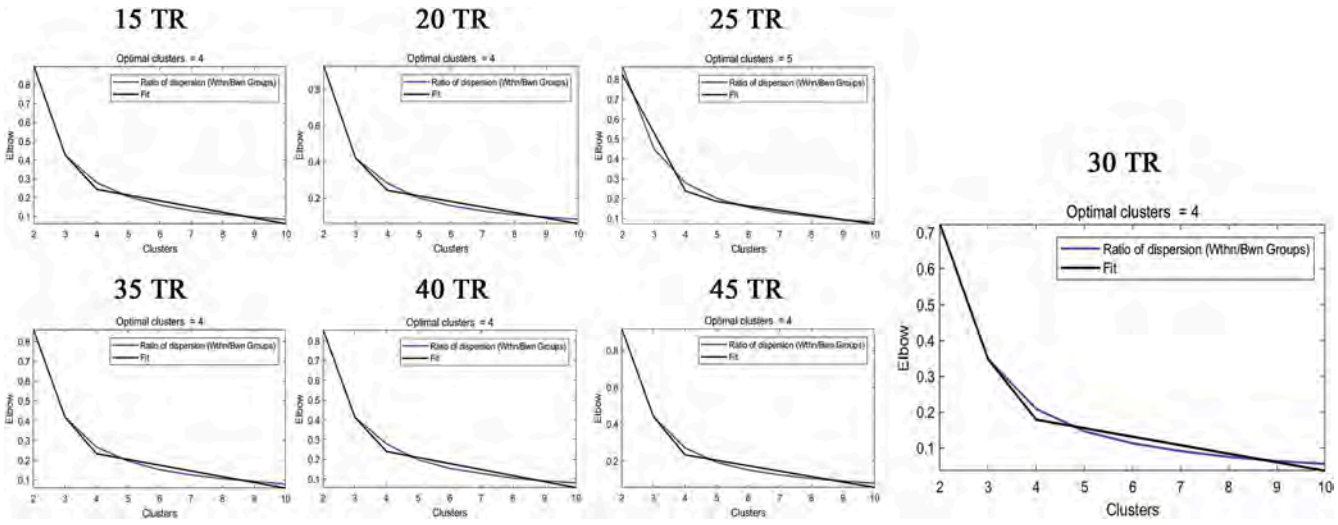

Fig. 3. The k-means results of different time window length (15TR, 20 TR, 25 TR, 30 TR, 35TR, 40 TR, 45 TR, respectively). The averaged window length of 30TR was the optimal window for the present study.

network. Using k-means clustering analysis, we identified four distinct dynamic brain states associated with different cognitive processing facets of the IER processing. Throughout the four brain states, the empathy network predominantly displayed connectivity with the cognitive control network and the affective generation network. Notably, the left MTG and VLPFC strongly mediate one's tendency and efficiency in utilizing IER, as well as the ultimate regulatory effects. These findings address the current research gap in understanding of cognitive-neural substrate of the dynamic IER processing.

The first brain state displayed connectivity patterns predominantly within the occipital lobe, temporal cortex and motor cortex. These areas encompass the visual network, the empathy network, and the affective generation network. Previous classical emotion regulation studies have shown these networks are integral to the rapid and spontaneous processing of affective information (Mellers, 2001). Specific areas in the occipital lobe, such as the cuneus and calcarine, have been identified as vital for processing visual information and recognizing objects (Schupp et al., 2003). Meanwhile, Reeck and colleagues introduced the IER cycle mode, grounded on Gross's model of cognitive control of emotion. This cycle initiates with the processing of affective stimuli (Reeck et al., 2016). Intriguingly, the brain state 1 reveals primary connectivity between the visual network and the affective generation network, suggesting that this initial state might reflect the early stages of visual affective stimuli processing, aligning with visual emotional stimuli processing at the first stage of the IER.

As the IER cycle progresses, it also encompasses the target's perception to the regulator. The phase involves focusing attention on various facets of both the initial emotional elicitor and the regulator (Reeck et al., 2016). In this study, the target receives and experiences the regulatory information by the regulator, which is proved as empathy processing of the target to the regulator. Our previous IER study demonstrates that the target's empathy ability is a crucial factor for the IER processing (Wang et al., 2023). Meanwhile, the empathy network, comprising the MTG, TPJ, dmPFC and precuneus has also been observed to be activated by the target in IER studies (Xie et al., 2016; Carmen et al., 2021). Indeed, the dFNC results reveal that the state 2 exhibits prominent connections spanning the temporal cortex, parietal cortex and temporal-parietal junction. These areas are associated with both the empathy network and the affective generation network, which are suggested to aid the target in perceiving the regulator's affective state and understanding the reappraisal stimuli (Bernhardt & Singer, 2012; Decety & Jackson, 2004). Specifically, the MTG is involved in the processing of facial information, social emotion recognition, and regions in the temporal and parietal areas that are implicated in visuospatial and semantic representation (Aggleton, 2000; Yun et al., 2017). Also, The MTG, a pivotal region is engaged in the empathetic decoding of others' affective states (Choi et al., 2016; Cremers et al., 2015). It worth to notice that, the degree centrality of the left MTG in the state 2 mediates the association between emotional ratings and one's tendency to use IER. As degree centrality reflects the quantity and strength of local network connections, while also highlighting a node's capacity to capture and disseminate stimulus information within a network (Zhang et al., 2016). It suggests that the left MTG shows central hub to dispatch emotion regulation related stimuli to other regions as well as this deployment contributes to the emotion regulation effects and enhances one's tendency to use IER. Collectively, the state 2 details the how the target empathy to the regulator to perceiving the regulatory information, and highlights the left MTG plays an essential role in empathy processing of the IER processing.

After perceiving relevant reappraisal features, the situation adjusts to modify its affective states, representing the cognitive change stage in general emotion regulation (Fang et al., 2020; Ochsner et al., 2012; W. Zhang et al., 2023). Numerous fMRI studies have shown that both the prefrontal and parietal cortexes are key regions involved in emotion

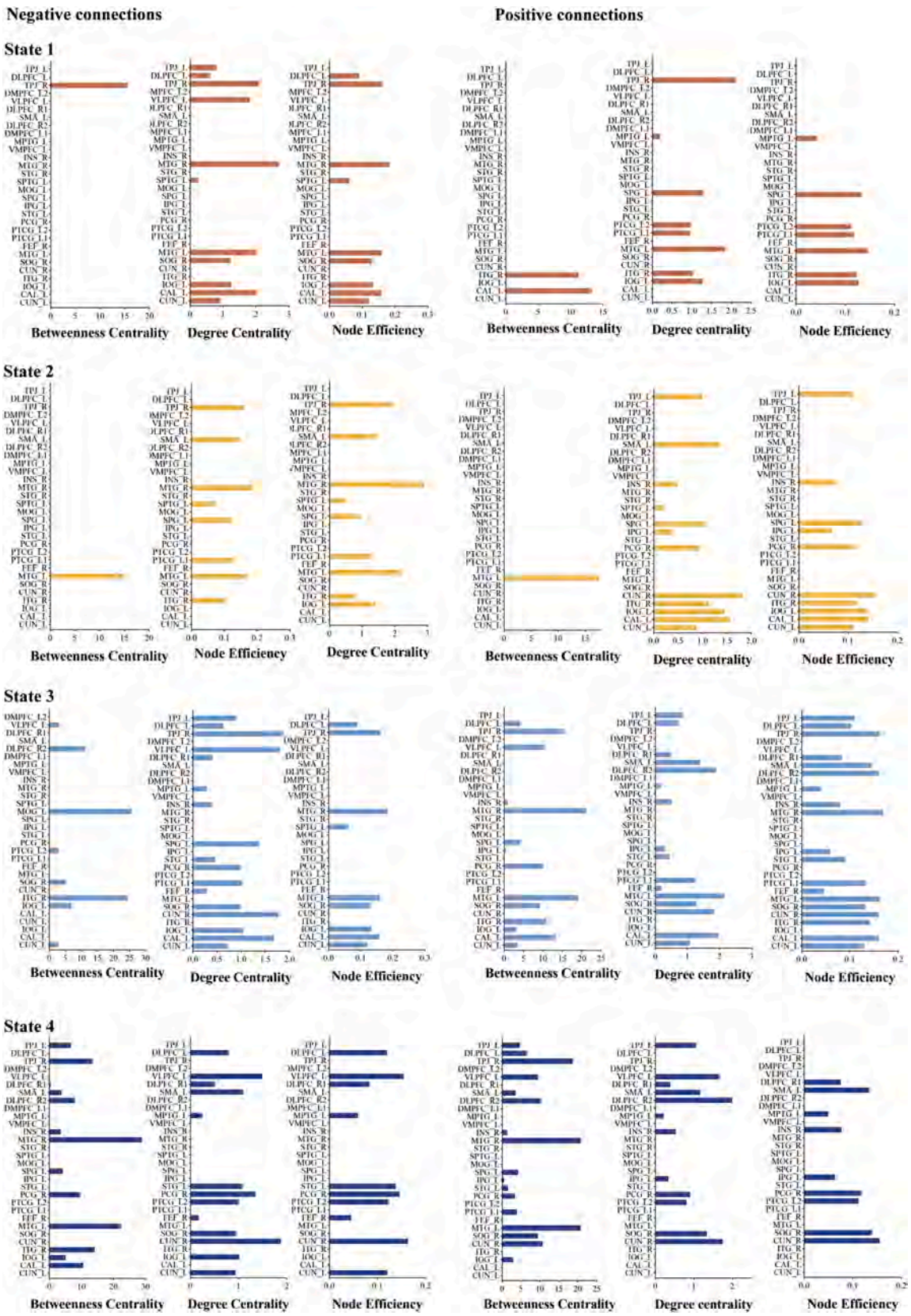

Fig. 4. a. The negative emotional rating of IER and watch conditions. b. The sFC of the IER processing under the group independent component analysis spatial map. c. The betweenness centrality, degree centrality and node efficiency of sFC in positive connections and negative connections (FDR, $p<0.01$). d. The correlation between behavioral performance and sFC properties.

Table 2
The functional connectivity in each distinct brain state of dFC (FDR, $p < 0.005$).

State 1		State 2		State 3		State 4	
ICs	*ICs*	*ICs*	*ICs*	*ICs*	*ICs*	*ICs*	*ICs*
MTG_L	CAL_L +	MTG_L	TPJ _L -	MTG_L	IPG_L -	MTG_L	PTCG_L +
	CUN_L +		TPJ _R -		STG_L -		PTCG_L +
	MOG_L +		PTCG_L +	MTG_R	IPG_L -		TPJ_L -
	SPTG_L -		SPG_L +		ITG_R +		TPJ_R -
	TPJ _R +		IOG_L +	STG_L	SPG_L +		ITG_R +
ITG_R	CAL_L +		IOG_L +		CAL_L +		STG_L -
	MOG_L +	MTG_R	TPJ _L -		IOG_L +		SOG_R +
	SPG_L +		TPJ _R -	ITG_R	PCG_R +		CUN_R -
STG_R	CUN_R +	ITG_R	SPG_L -	DLPFC _L	FEF_R +	MTG_R	TPJ _R -
VMPFC_L	STG_L +	MPTG_L	IOG_L +		VLPFC_L +		SMA_L -
	MTG_L +	SPTG_L	SMA_L -	DLPFC _R1	CUN_L -		IPG_L -
VLPFC_L	TPJ _R -	FEF_R	PTCG_L +	DLPFC_R2	FEF_R +		CUN_R -
	IOG_L -	SPG_L	TPJ_R +		STG_L +		ITG_R +
SPTG_L	TPJ _L +			VLPFC _L VMPFC	FEF_R +	ITG_R	CUN_L +
	SOG_R -			VMPFC_L	STG_L +	DLPFC_L	SMA_L -
INS_R	CUN_R +			DMPFC_L1	STG_L +	DLPFC_R2	TPJ_R +
	MOG_L +			FEF_R	IOG_L +		MTG_R -
FEF_R	TPJ _R +				TPJ _R +	DMPFC_L1	MTG_R -
	IPL_L +				PTCG_L -		CUN_R +
CAL_L	SPG_L +			TPJ _R	CAL_L +	DMPFC_L2	MTG_R -
	TPJ _L -			IPG_L	CAL_L +	TPJ_R	ITG_R +
	CUN_R -				IOG_L +		CAL_L +
IOG_L	MOG_L +				ITG_R +		IOG_L +
	IPL_L +						SPG_L +
MOG_L	CUN_R -					TPJ_L	ITG_R +
							CAL_L +
						INS_R	SOG_R -
						PTCG_L	IOG_L -
						MOG_L	PTCG_L +

Note. The " + " represents positive connections, the " - " represents negative connections. DLPFC (dorsolateral prefrontal cortex); VLPFC (ventrolateral prefrontal cortex); VMPFC (ventromedial prefrontal cortex); DMPFC (dorsomedial prefrontal cortex); L (left); R (right); ICs (independent components). SMA (supplementary motor area); IPG (inferior parietal gyrus); SPG (parietal superior gyrus); TPJ (temporal parietal junction); CUN (cuneus); IOG (inferior occipital gyrus); MOG (middle occipital gyrus); SOG (superior occipital gyrus); CAL (calcarine lobe); ITG (inferior temporal gyrus); MTG (middle temporal gyrus); STG (superior temporal gyrus); SPTG (superior pole temporal gyrus); INS (insula). FEF (frontal eye fields); PTCG (postcentral gyrus).

regulation (Dorfel et al., 2014; Morawetz et al., 2017; Kohn et al., 2014). Our findings for the state 3 highlight dominant connectivity among the DLPFC, VLPFC, TPJ, IPL, STS, and MTG. A prevailing model posits a 'top-down' system, where the DLPFC and VLPFC play pivotal roles in focusing attention on reappraisal goals to the affective generation network (Ochsner et al., 2012). Research has found the VLPFC enhanced connections to goal-specific processing regions in higher-order areas that support the top-down modulation of task-relevant processes (Brosnan & Wiegand, 2017; Zhao et al., 2020). Additionally, the distinct aspect of the IER, compared to general emotion regulation, with emphasis on social communication (Reeck et al., 2016). This implies that in the context of the IER processing, the temporal region, which plays a pivotal role in empathy, also holds significant importance during the executive regulation stage. In fact, the VLPFC and MTG displayed high centrality and efficiency regions, as well as positive correlation with IER tendency and efficiency in this state. Importantly, the betweenness centrality of left VLPFC mediates the association between IRQ tendency and the effects of IER. As the betweenness centrality quantifies the degree to which a node serves as a crucial link connecting various nodes within the network. Nodes exhibiting high betweenness centrality are deemed pivotal for facilitating communication and integration among distinct brain regions. It suggests that the left VLPFC integrate the regulation stimuli and transfer this information to other regions in cognitive change stage. Furthermore, this integration and transferring of the VLPFC mediates one's efficiency of the IER deployment and the effects of IER. The certain neural dynamic characteristics of MTG and VLPFC mediate the relationship between measures of trait IER and the emotional reappraisal effect after encountering an emotional stimulus. Overall, these findings suggest that top-down affective modulation is based on cognitive control network as well as empathy network. This is especially true for the left VLPFC in cognitive change stage of the IER processing.

The final brain state shows predominant associations in the empathy network, and the affective generation network, particularly highlighting dominant connections of DLPFC with TPJ/temporal cortex and INS-temporal cortex. The TPJ's has been noted for processing internally generated information (Bzdok et al., 2013; Kanske et al., 2015). Bzdok and colleagues show that the connectivity of TPJ and DLPFC extends to both the temporal gyrus, as observed during the retrieval of episodic and semantic processing (Bzdok et al., 2013). DLPFC and temporal cortex appear to function as a semantic cognition network with lateral temporal cortex involved in the semantic representation of information (Hodges et al., 1992; Thompson-Schill et al., 1997; Whitney et al., 2011). Moreover, both anatomical and resting-state functional studies have determined that the insula is interconnected with the temporal cortex (Flynn, 1999; Cauda et al., 2011). The somatosensory inputs may, through the projection to the insula from temporal cortex reach insula and then the insula sends projection to amygdala (Schneider et al., 1993). From this perspective, the functional connectivity between the temporal cortex and the insula in the present study indicates the flow of emotional information processing. This is consistent with the IER processing, the target retrieves emotion regulation memories to modulate their negative emotions. Both the insula and temporal pole, established as crucial regions in the affective generation network, are thought to play roles in awareness of internal physiological states and socioemotional processing (Critchley, 2004; Olson, 2007). The insula, in particular, represents a viscerotopic map of ascending sensory inputs from the body and is implicated in negative affective experiences (Wager, 2017; Craig, 2009). Collectively, these findings imply that the modulation of affective response in the IER processing hinges on the interplay between

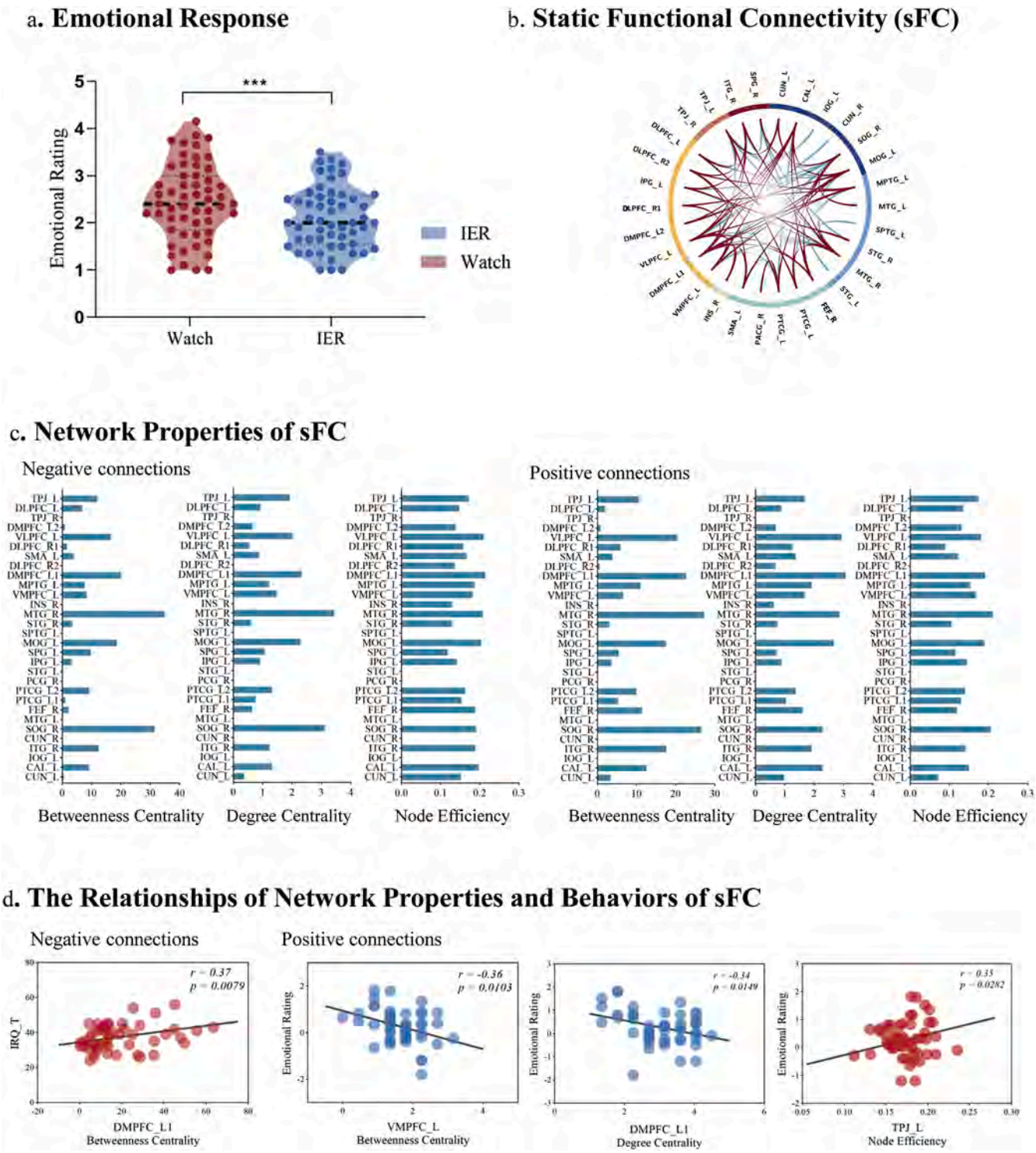

Fig. 5. The betweenness centrality, degree centrality and node efficiency of dFC in positive connections and negative connections (FDR, $p < 0.01$).

the cognitive control network and the empathy network. This then interacts with the retrieval of reappraisal stimuli and influences the down-regulation of negative emotions in the response modulation stage of the IER processing.

5. Limitations

Although the present investigation provides insight into the sFNC and dFNC of the IER processing, the acknowledgements of some limitations are imperative. While the study was conducted using fMRI equipment, with limited temporal resolution, may encounter accurate characterization of the rapidly evolving processing of the IER processing. Therefore, future explorations could investigate multiple modalities to delve deeper into the IER processing. Also, the current study focuses on the cognitive-neural mechanism in perspective of the "target", with less emphasis for the "regulator". However, the regulator plays an important role in IER processing, thus simultaneous inclusion and analysis of both target and regulator could improve the IER. Thus, the further investigation should consider the influence of the "regulator" in the IER processing.

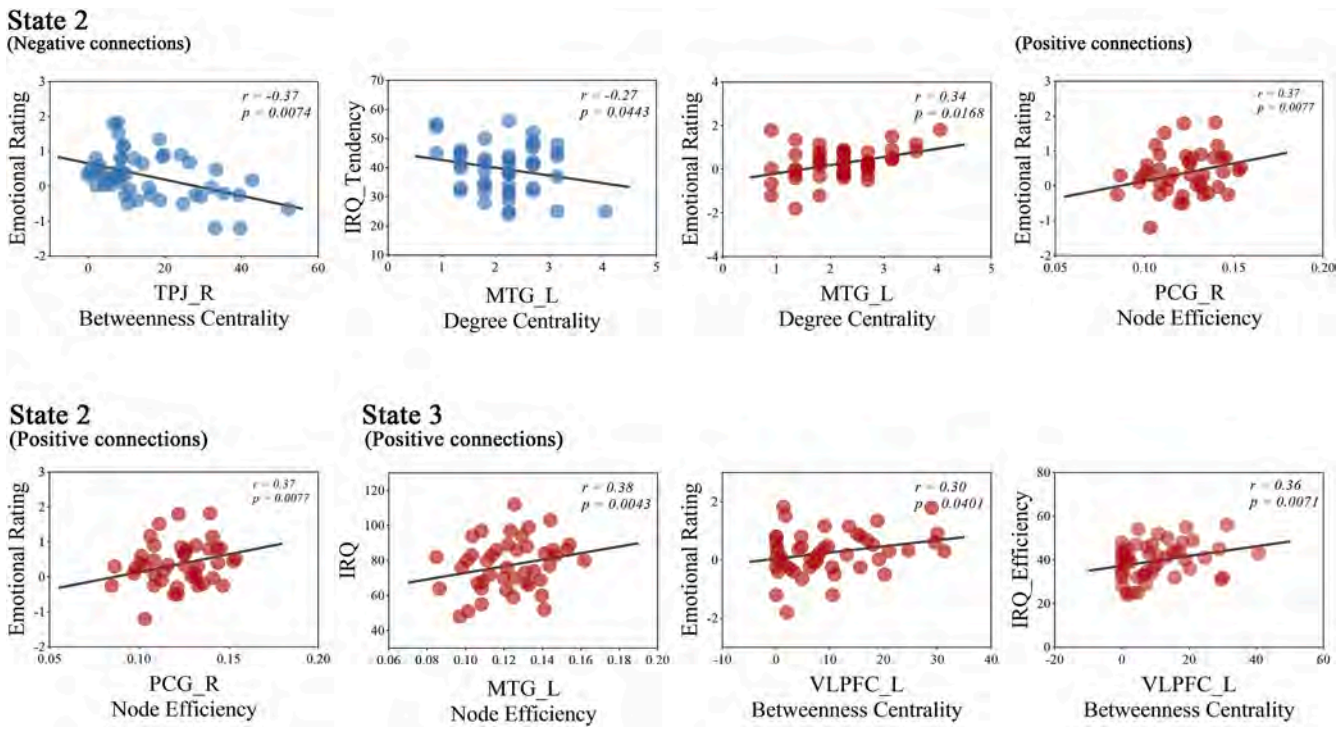

Fig. 6. The correlation of graphic theoretical property and behaviors in positive connections and negative connections of each brain state.

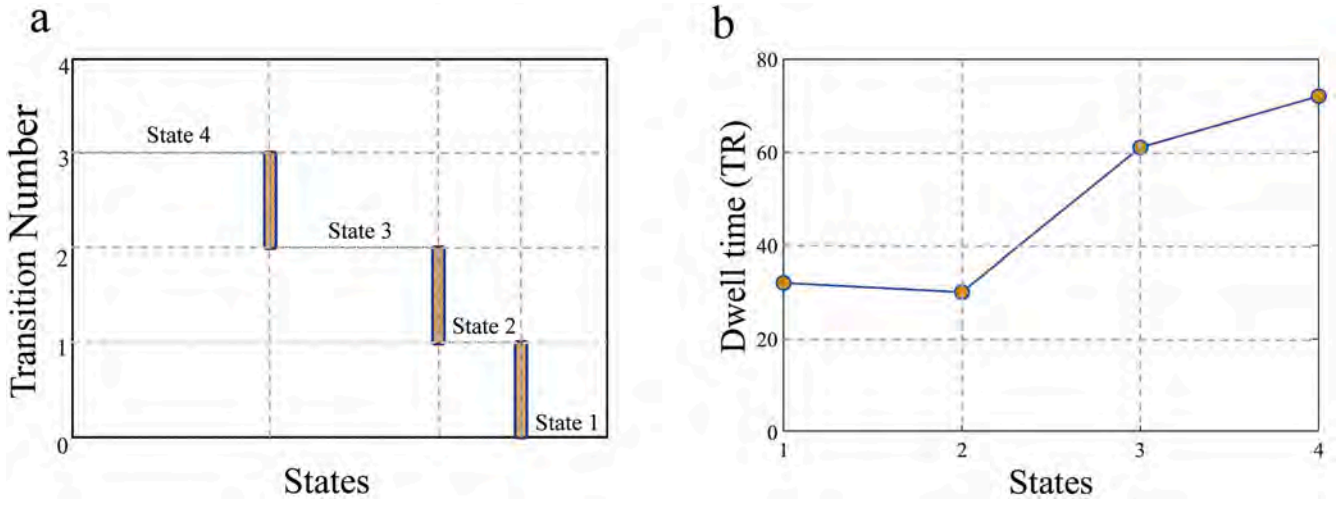

Fig. 7. State vectors, a) number of transition for dynamic brain states, b) dwell time for entire duration of each state.

6. Conclusion

By employing sliding window approach, this study has provided insight into the dynamics of emotion regulation, showing distinct functional network connectivity states during the processing of IER. Four unique brain states were identified, each associated with a domain network profiling the dynamic cognitive processing throughout the IER. The empathy network's key hubs, specifically the left MTG, playing pivotal role in encouraging one's IER-seeking tendency, as well as the IER effects. Meanwhile, the left DLPFC pivots one's efficiency of IER. The aforementioned discoveries offer valuable insights into the intricate cognitive and neural substrates that underlie the dynamic IER processing. They are pertinent to our comprehension of affective disorders, such as the diminished susceptibility to IER observed in individuals with social anxiety and depression.

Funding

This work was supported by the National Natural Science Foundation of China NSFC82250410380, NSFC62171101)

CRediT authorship contribution statement

Jiazheng Wang: Writing – review & editing, Writing – original draft, Investigation, Formal analysis, Data curation, Conceptualization. **Zhenzhen Yang:** Validation, Software, Resources, Formal analysis, Data curation. **Benjamin Klugah-Brown:** Writing – review & editing, Supervision, Formal analysis. **Tao Zhang:** Writing – review & editing, Formal analysis. **Jiemin Yang:** Writing – review & editing, Conceptualization. **JiaJin Yuan:** Writing – review & editing, Supervision, Project administration, Investigation, Conceptualization. **Bharat B Biswal:**

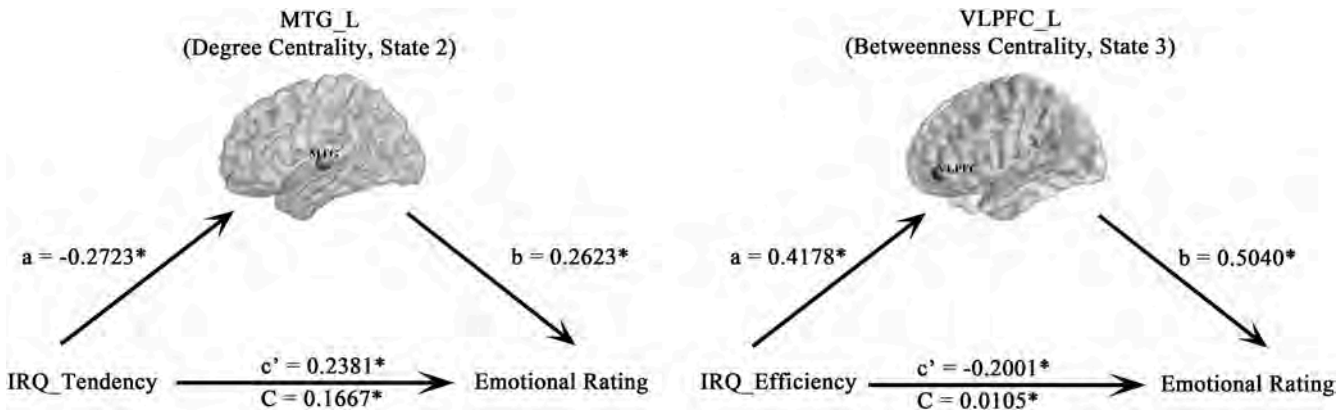

Fig. 8. The mediation results among emotional rating; IRQ_Efficiency (interpersonal regulation questionnaire_efficiency), IRQ_Tendency (interpersonal regulation questionnaire_tendency); betweenness centrality of the left VLPFC and degree centrality of the left MTG in state 2 and state 3.

Writing – review & editing, Supervision, Project administration, Methodology, Investigation, Funding acquisition, Conceptualization.

Declaration of competing interest

The authors have declared that there are no conflicts of interest in relation to the subject of this study.

Data availability

Data will be made available on request.

Supplementary materials

Supplementary material associated with this article can be found, in the online version, at doi:10.1016/j.neuroimage.2024.120789.

References

Aggleton, J.P., 2000. The amygdala: A functional analysis [M]. Oxford University Press.

Allen, E.A., Damaraju, E., Plis, S.M., Erhardt, E.B., Eichele, T., Calhoun, V.D., 2014. Tracking whole-brain connectivity dynamics in the resting state. Cerebr. Cortex 24 (3), 663–676.

Bassett, D.S., Wymbs, N.F., Porter, M.A., Mucha, P.J., Carlson, J.M., Grafton, S.T., 2011. Dynamic reconfiguration of human brain networks during learning. Proc. Natl. Acad. Sci. 108 (18), 7641–7646.

Benedek Kurdi Lozano, S., Banaji, M.R., 2017. Introducing the Open Affective Standardized Image Set (OASIS). Behav. Res. Methods 49 (2), 457–470. https://doi.org/10.3758/s13428-016-0715-3. PMID: 26907748.

Bernhardt, B.C., Singer, T., 2012. The neural basis of empathy. Annu Rev. Neurosci. 35, 1–23.

Bertolero, M., Bassett, D., 2020. On the nature of explanations offered by network science: A perspective from and for practicing neuroscientists. Top. Cogn. Sci. 12 (4), 1272–1293.

Brosnan, M.B., Wiegand, I., 2017. The dorsolateral prefrontal cortex, a dynamic cortical area to enhance top-down attentional control. J. Neurosci. 37 (13), 3445–3446.

Butler, E.A., 2011. Temporal interpersonal emotion systems: The "TIES" that form relationships. Personal. Soc. Psychol. Rev. 15 (4), 367–393.

... Bzdok, D., Langner, R., Schilbach, L., Jakobs, O., Roski, C., Caspers, S., Eickhoff, S.B., 2013. Characterization of the temporo-parietal junction by combining data-driven parcellation, complementary connectivity analyses, and functional decoding Neuroimage 81, 381–392. https://doi.org/10.1016/j.neuroimage.2013.05.046.

Choi, S.H., Shin, J.E., Ku, J., Kim, J.J., 2016. Looking at the self in front of others: Neural correlates of attentional bias in social anxiety. J. Psychiatr. Res. (75-) 75.

Coan, J.A., Schaefer, H.S., Davidson, R.J., 2006. Lending a hand: Social regulation of the neural response to threat. Psychol. Sci. 17 (12), 1032–1039.

Cremers, H.R., Veer, I.M., Spinhoven, P., Rombouts, S.A.R.B., Yarkoni, T., Wager, T.D., Roelofs, K., 2015. Altered cortical-amygdala coupling in social anxiety disorder during the anticipation of giving a public speech. Psychol. Med. 45 (07), 1521–1529.

Decety, J., Jackson, P.L., 2004. The functional architecture of human empathy. Behav. Cogn. Neurosci. Rev. 3 (2), 71–100.

Dixon-Gordon, K.L., Bernecker, S.L., Christensen, K., 2015. Recent innovations in the field of interpersonal emotion regulation. Curr. Opin. Psychol. 3, 36–42.

Dorfel, D., Lamke, J.P., Hummel, F., Wagner, U., Erk, S., Walter, H., 2014. Common and differential neural networks of emotion regulation by Detachment, Reinterpretation, Distraction, and Expressive Suppression: A comparative fMRI investigation. Neuroimage 101, 298–309.

Douw, L., Quaak, M., Fitzsimmons, S.M., de Wit, S.J., van der Werf, Y.D., van den Heuvel, O.A., Vriend, C., 2020. Static and dynamic network properties of the repetitive transcranial magnetic stimulation target predict changes in emotion regulation in obsessive-compulsive disorder. Brain Stimul. 13 (2), 318–326.

Fang, F., Potter, T., Nguyen, T., Zhang, Y., 2020. Dynamic reorganization of the cortical functional brain network in affective processing and cognitive reappraisal. Int. J. Neural Syst. 30 (10), 2050051.

Gao, W., Biswal, B., Chen, S., Wu, X., Yuan, J., 2021. Functional coupling of the orbitofrontal cortex and the basolateral amygdala mediates the association between spontaneous reappraisal and emotional response. Neuroimage 232, 117918.

Hofmann, S.G., 2014. Interpersonal emotion regulation model of mood and anxiety disorders. Cognit. Ther. Res. 38, 483–492.

Hutchison, R.M., Womelsdorf, T., Allen, E.A., Bandettini, P.A., Calhoun, V.D., Corbetta, M., Gonzalez-Castillo, J., 2013. Dynamic functional connectivity: Promise, issues, and interpretations. Neuroimage 80, 360–378.

Hutchison, R.M., Womelsdorf, T., Gati, J.S., Everling, S., Menon, R.S., 2013. Resting-state networks show dynamic functional connectivity in awake humans and anesthetized macaques. Hum. Brain Mapp. 34 (9), 2154–2177.

Jauniaux, J., Khatibi, A., Rainville, P., Jackson, P.L., 2019. A meta-analysis of neuroimaging studies on pain empathy: Investigating the role of visual information and observers' perspective. Soc. Cogn. Affect. Neurosci. 14 (8), 789–813.

Johnstone, T., Van Reekum, C.M., Urry, H.L., Kalin, N.H., Davidson, R.J., 2007. Failure to regulate: Counterproductive recruitment of top-down prefrontal-subcortical circuitry in major depression. J. Neurosci. 27 (33), 8877–8884.

Kuang, L.D., Li, H.Q., Zhang, J., Gui, Y., Zhang, J., 2024, February 26. Dynamic functional network connectivity analysis in schizophrenia based on a spatiotemporal CPD framework. J. Neural Eng. 21 (1). https://doi.org/10.1088/1741-2552/ad27ee. PMID: 38335544.

Klugah-Brown, B., Luo, C., He, H., Jiang, S., Armah, G.K., Wu, Y., Yao, D., 2019. Altered dynamic functional network connectivity in frontal lobe epilepsy. Brain Topogr. 32, 394–404.

Koenigsberg, H.W., Fan, J., Ochsner, K.N., Liu, X., Guise, K.G., Pizzarello, S., Goodman, M., 2009. Neural correlates of the use of psychological distancing to regulate responses to negative social cues: A study of patients with borderline personality disorder. Biol. Psychiatry 66 (9), 854–863.

Liang, X., Pang, X., Zhao, J., Yu, L., Wu, P., Li, X., Zheng, J., 2021. Altered static and dynamic functional network connectivity in temporal lobe epilepsy with different disease duration and their relationships with attention. J. Neurosci. Res. 99 (10), 2688–2705.

Mellers, A. (2001). Emotion regulation in adulthood: timing is everything.

Menatti, A.R., DeBoer, L.B., Weeks, J.W., Heimberg, R.G., 2015. Social anxiety and associations with eating psychopathology: mediating effects of fears of evaluation. Body. Image 14, 20–28. https://doi.org/10.1016/j.bodyim.2015.02.003.

Morawetz, C., Berboth, S., Bode, S., 2021. With a little help from my friends: The effect of social proximity on emotion regulation-related brain activity. Neuroimage 230, 117817.

Morawetz, C., Bode, S., Derntl, B., Heekeren, H.R., 2017. The effect of strategies, goals and stimulus material on the neural mechanisms of emotion regulation: A meta-analysis of fMRI studies. Neurosci. Biobehav. Rev 72, 111–128.

Morawetz, C., Riedel, M.C., Salo, T., Berboth, S., Eickhoff, S.B., Laird, A.R., Kohn, N., 2020. Multiple large-scale neural networks underlying emotion regulation. Neurosci. Biobehav. Rev. 116, 382–395.

N, Kohn, S, B., Eickhoff, M., Scheller, Fox, 2014. Neural network of cognitive emotion regulation — An \\{ALE\\} meta-analysis and \\{MACM\\} analysis. Neuroimage.

Nomi, J.S., Farrant, K., Damaraju, E., Rachakonda, S., Calhoun, V.D., Uddin, L.Q., 2016. Dynamic functional network connectivity reveals unique and overlapping profiles of insula subdivisions. Hum. Brain Mapp. 37 (5), 1770–1787.

Ochsner, K.N., Ray, R.D., Cooper, J.C., Robertson, E.R., Chopra, S., Gabrieli, J.D.E., Gross, J.J., 2004. For better or for worse: Neural systems supporting the cognitive down- and up-regulation of negative emotion. Neuroimage 23, 483–499.

Ochsner, K.N., Silvers, J.A., Buhle, J.T., 2012. Functional imaging studies of emotion regulation: A synthetic review and evolving model of the cognitive control of emotion. Ann. N. Y. Acad. Sci. 1251 (1), E1–E24.
Raghavan Unnithan, S.K., Kannan, B., Jathavedan, M., 2014. Betweenness centrality in some classes of graphs. Int. J. Combinator. 2014.
Reeck, C., Ames, D.R., Ochsner, K.N., 2016. The social regulation of emotion: An integrative, cross-disciplinary model. Trends. Cogn. Sci. 20 (1), 47–63.
Schoonheim, M.M., Douw, L., Broeders, T.A., Eijlers, A.J., Meijer, K.A., Geurts, J.J., 2021. The cerebellum and its network: Disrupted static and dynamic functional connectivity patterns and cognitive impairment in multiple sclerosis. Multiple Sclerosis J. 27 (13), 2031–2039.
Schupp, H.T., Markus, J., Weike, A.I., Hamm, A.O., 2003. Emotional facilitation of sensory processing in the visual cortex. Psychol. Sci. 14 (1), 7–13.
Wager, T.D., Davidson, M.L., Hughes, B.L., Lindquist, M.A., Ochsner, K.N., 2008. Prefrontal-subcortical pathways mediating successful emotion regulation. Neuron 59 (6), 1037–1050.
Wang, J., Yang, J., Yang, Z., Gao, W., Zhang, H., Ji, K., Biswal, B.B., 2023. Boosting interpersonal emotion regulation through facial imitation: Functional neuroimaging foundations. Cereb. Cortex. https://doi.org/10.1093/cercor/bhad402.
Wang, S., Du, Y., Deng, Y., 2017. A new measure of identifying influential nodes: Efficiency centrality. Commun. Nonlin. Sci. Numer. Simul. 47, 151–163.
Williams, W.C., Morelli, S.A., Ong, D.C., Zaki, J., 2018. Interpersonal emotion regulation: Implications for affiliation, perceived support, relationships, and well-being. J. Pers. Soc. Psychol. 115 (2), 224.
Xie, X., Bratec, S.M., Schmid, G., Meng, C., Doll, A., Wohlschläger, A., Pekrun, R., 2016. How do you make me feel better? Social cognitive emotion regulation and the default mode network. Neuroimage 134, 270–280.
Yun, J.Y., Kim, J.C., Ku, J., Shin, J.E., Kim, J.J., Choi, S.H., 2017. The left middle temporal gyrus in the middle of an impaired social-affective communication network in social anxiety disorder. J. Affect. Disord. 214 (Complete), 53–59.
Zaki, J., 2020. Integrating empathy and interpersonal emotion regulation. Annu. Rev. Psychol. 71, 517–540.
Zaki, J., Williams, W.C., 2013. Interpersonal emotion regulation. Emotion. 13 (5), 803.
Zhang, T., Liu, T., Li, F., Li, M., Liu, D., Zhang, R., Luo, C., 2016. Structural and functional correlates of motor imagery BCI performance: Insights from the patterns of fronto-parietal attention network. Neuroimage 134, 475–485.
Zhang, W., Qiu, L., Tang, F., Li, H., 2023. Affective or cognitive interpersonal emotion regulation in couples: An fNIRS hyperscanning study. Cerebral cortex 33 (12), 7960–7970.
Zhao, J., Mo, L., Bi, R., He, Z., Zhang, D., 2020. The VLPFC versus the DLPFC in Downregulating Social Pain Using Reappraisal and Distraction Strategies. The Journal of Neuroscience 41 (6). JN-RM-1906-1920.